Dip-Moveout Processing by Fourier Transform in Anisotropic Media

John Anderson and Ilya Tsvankin

ABSTRACT

Conventional dip-moveout (DMO) processing is designed for isotropic media and cannot handle angle-dependent velocity. We show that Hale's isotropic DMO algorithm remains valid for elliptical anisotropy but may lead to severe errors for non-elliptical transversely isotropic models, even if velocity anisotropy is moderate.

Here, we present an extension of Hale's constant-velocity DMO method to anisotropic media. The DMO operator, to be applied to normal-moveout-corrected data, is based on the analytic expression for normal moveout velocity for dipping reflectors given by Tsvankin (1993). Since the anisotropic DMO depends on the elastic parameters of the medium, it should be preceded by an inversion procedure designed to obtain the NMO velocity as a function of ray parameter. This inversion technique for transversely isotropic media is discussed in detail by Alkhalifah and Tsvankin (1994). Another complication introduced by anisotropy is the influence of nonhyperbolic moveout not accounted for in our DMO operator. However, for relatively short spreads typical for conventional acquisition design, deviations from hyperbolic moveout are not significant. Moreover, the distortions due to nonhyperbolic moveout become less pronounced with increasing reflector dip.

Impulse responses and synthetic examples for typical transversely isotropic models with a vertical symmetry axis (VTI) demonstrate the accuracy and efficiency of the new DMO technique. It should be emphasized that once the inversion step has been completed, the proposed NMO-DMO sequence does not take any more computing time than that for Hale's method in isotropic media. Our anisotropic DMO operator is not limited to VTI media; it can be applied in the same fashion in symmetry planes of more complicated models such as orthorhombic. Also, the algorithm can be generalized to handle an inhomogeneous overburden by replacing the single-layer NMO formula with a more general equation for layered media developed by Alkhalifah and Tsvankin (1994).

INTRODUCTION

Seismic anisotropy has been widely recognized as a property of many subsurface formations of different origin. For instance, existing data suggest that shales are

often transversely isotropic with substantial velocity anisotropy in the vertical plane (White et al., 1983; Robertson and Corrigan, 1983; Banik, 1984; Sams et al., 1993, among others).

Anisotropy may have a strong influence on all seismic processing methods including dip-moveout algorithms (Levin, 1990; Larner, 1993; Tsvankin, 1993). Most constant-velocity DMO techniques are based on the cosine-of-dip dependence of moveout velocity on reflector dip valid for homogeneous isotropic media (Levin, 1971):

$$V_{\rm nmo}(\phi) = V_{\rm nmo}(0)/\cos\phi\,, \tag{1}$$

where $V_{\rm nmo}$ is moveout velocity, and ϕ is the dip angle. Reflection moveout in a homogeneous isotropic medium is purely hyperbolic, and equation (1) remains accurate even for long spreads. Clearly, formula (1) cannot be expected to hold if the velocity above the reflector becomes angle-dependent.

Tsvankin (1993) (hereafter referred to as Paper I) derived an analytic equation for normal moveout velocity for dipping reflectors in anisotropic media and studied the error of equation (1) for transversely isotropic models. He concluded that the dip-dependence of the P-wave moveout velocity for transverse isotropy with a vertical symmetry axis (VTI media) is controlled, to a significant degree, by the difference between the parameters ϵ and δ introduced by Thomsen (1986). If $\epsilon - \delta > 0$ (the most common case), the cosine-of-dip corrected moveout velocity may be significantly larger than the moveout velocity for a horizontal reflector. Even for moderate values of $\epsilon - \delta = 0.1$ and $\epsilon \leq 0.2$, the error of the isotropic equation (1) reaches 25 percent at 45 deg dip and 30-35 percent at a dip of 60 deg. For a larger difference $\epsilon - \delta = 0.2$, the moveout velocity at 60 deg dip after the cosine-of-dip correction remains almost 60 percent higher than the zero-dip moveout velocity.

Another conclusion drawn in Paper I is that for inhomogeneous transversely isotropic media with positive values of the difference $\epsilon - \delta$ and a linear increase in the vertical velocity with depth, inhomogeneity reduces the error in constant-velocity DMO caused by anisotropy. However, in the absence of a substantial velocity gradient, conventional constant-velocity DMO algorithms can be expected to lead to errors in typical transversely isotropic media.

Since dip-moveout removal represents an important step in the conventional processing flow (NMO-DMO-poststack migration), any errors in DMO will propagate into the final seismic image. Clearly, there is a need to develop dip-moveout algorithms capable of handling transversely isotropic media and, in the future, more complicated anisotropic models. Uren et al. (1990) showed that Forel-Gardner DMO (1988) can be updated and applied in a straightforward way to elliptically anisotropic models. However, elliptical anisotropy is no more than a special case of transverse isotropy that corresponds to $\epsilon = \delta$ and cannot be considered as typical for real rocks (Thomsen, 1986). Also, Paper I demonstrates that the P-wave DMO correction is highly sensitive to deviations from elliptical anisotropy.

The main difficulty in devising efficient DMO algorithms for anisotropic media was the absence of closed-form expressions for normal moveout velocity necessary to replace the isotropic NMO formula (1). This gap was filled by the NMO equation from Paper I, which can be used in symmetry planes of anisotropic media. Here, we apply this equation to extend the dip-moveout method developed by Hale (1984) to anisotropic media. We show that the anisotropic correction to the Hale's DMO operator is mostly dependent on the difference $\epsilon - \delta$ and can make a significant contribution to DMO processing for non-elliptical models. In addition to NMO correction, the anisotropic DMO should be preceded by an inversion procedure intended to tabulate the NMO velocity as a function of ray parameter. We study the complications caused by anisotropy in the DMO process and illustrate the performance of our algorithm by calculating impulse responses and processing synthetic sections for typical transversely isotropic models.

ANALYTIC FORMULATION

Hale's DMO method

First, we review the fundamentals of Hale's (1984) DMO algorithm. If the medium is isotropic, the moveout curve for a dipping reflector is a hyperbola parametrized by the NMO velocity (1).

$$t^2 = t_0^2 + \frac{4h^2}{V_{\rm nmo}^2(\phi)}\,, \tag{2}$$

where t is the original event time, t_0 is the two-way traveltime on the zero-offset section from the common-midpoint position and h is the half offset. We also use the normal-moveout equation for horizontal reflectors that is applied to the data prior to DMO processing.

$$t^2 = t_n^2 + \frac{4h^2}{V_{\rm nmo}^2(0)}\,, \tag{3}$$

where t_n is the normal-moveout-corrected time. Combining equations (2) and (3) yields an expression for the zero-offset time in terms of the NMO-corrected time.

$$t_0^2 = t_n^2 + 4h^2\left[\frac{1}{V_{\rm nmo}^2(0)} - \frac{1}{V_{\rm nmo}^2(\phi)}\right]. \tag{4}$$

This equation, valid both in isotropic media and for the hyperbolic portion of the moveout curve in anisotropic media, is required for the coordinate transformation used in Hale's DMO.

In a homogeneous, isotropic medium, we have from equation (1)

$$t_0^2 = t_n^2 + 4h^2\left[\frac{1}{V_{\rm nmo}^2(0)} - \frac{\cos^2(\phi)}{V_{\rm nmo}^2(0)}\right] = t_n^2 + \frac{4h^2\sin^2\phi}{V_{\rm nmo}^2(0)}\,. \tag{5}$$

In DMO processing it is more convenient to represent NMO velocity as a function of the ray parameter $p(\phi)$ (horizontal slowness) corresponding to the zero-offset reflection.

$$p(\phi) = \frac{1}{2}\frac{dt_0}{dy_0} = \frac{\sin\phi}{V} = \frac{k}{2\omega}\,, \tag{6}$$

where t_0 is the two-way traveltime on the zero-offset section $t_0(y_0)$, V is the velocity, k is the horizontal spatial wavenumber over the common-midpoint axis, and ω is the angular frequency associated with t_0.

Taking into account that in a homogeneous isotropic medium $V_{\rm nmo}(0)$ is equal to the true velocity V and introducing the ray parameter (6), the moveout equation (5) can be rewritten as

$$t_0^2 = t_n^2 + 4h^2p^2\,. \tag{7}$$

Hale's isotropic DMO corrects for the remaining dip-dependent moveout term ($4h^2p^2$). The process of generating the zero-offset section is split into the NMO and DMO steps with the DMO operator being completely independent of velocity.

Hale's DMO algorithm uses the following Fourier-transform relationships between the time-space domain and the frequency-wavenumber domain for the zero-offset wavefield P_0.

$$P_0(t_0, y_0, h) = \int \frac{d\omega}{2\pi} \int \frac{dk}{2\pi} P_0(\omega, k, h) e^{-i(\omega t_0 - k y_0)}\,; \tag{8}$$

$$P_0(\omega, k, h) = \int dt_0 \int dy_0 P_0(t_0, y_0, h) e^{i(\omega t_0 - k y_0)}\,. \tag{9}$$

We define the data after normal-moveout correction as $P_n(t_n, y_n, h)$, establish the relation between the zero-offset and common-offset NMO-corrected data as $P_0(t_0, y_0, h) \equiv P_n(t_n, y_n, h)$, and change variables accordingly.

In Hale's (1984) original algorithm, it is also assumed that $y_0 \equiv y_n$. A similar assumption is made in Paper I in the derivation of the equation (17) for $V_{\rm nmo}(\phi)$ in anisotropic media. The identification $y_0 \equiv y_n$ is not used by the "true amplitude" isotropic DMO methods discussed below. However, the only refinement due to a more accurate treatment of the relation between y_0 and y_n for isotropic DMO is a more complicated Jacobian for the coordinate transformations.

Substituting $P_n(t_n, y_n, h)$ into equation (9) yields

$$P_0(\omega, k, h) = \int dt_0 \int dy_0 P_n(t_n, y_n, h) e^{i(\omega t_0 - k y_0)}\,, \tag{10}$$

and

$$P_0(\omega, k, h) = \int dt_n \int dy_n P_n(t_n, y_n, h) J_T e^{i(\omega t_n A - k y_n)}\,, \tag{11}$$

where Hale defines $t_0 = t_n A$. To emphasize the form that we will use for the anisotropic equations, we write the term A in equation (11) as follows.

$$A = \sqrt{1 + \frac{4h^2}{t_n^2}\left[\frac{1}{V_{\rm nmo}^2(0)} - \frac{1}{V_{\rm nmo}^2(p)}\right]}\,. \tag{12}$$

Finally, we use the isotropic relationships to put A in the form used by Hale (1984).

$$A = \sqrt{1 + \frac{4h^2p^2}{t_n^2}} = \sqrt{1 + \frac{k^2h^2}{\omega^2 t_n^2}}. \tag{13}$$

The Jacobian J_T of the transformation (11) in the original Hale's algorithm is defined as

$$J_T = \frac{\partial t_0}{\partial t_n} = \frac{t_n}{t_0} = A^{-1}\,. \tag{14}$$

Two "true-amplitude" variants of Hale's algorithm are of interest. Both correct Hale's identification $y_0 \equiv y_n$, make the corresponding correction to the t_0 as defined in equation (2), and thereby honor the movement of the surface location associated with a specular reflection point during the transformation to zero offset. The phase factors in equation (11) used by these "true-amplitude" algorithms coincide with Hale's phase factor; each differs from the original Hale's algorithm only in the value assumed for J_T. Both require a Jacobian based on $\frac{\partial(t_0,y_0)}{\partial(t_n,y_n)}$ rather than Hale's more simple Jacobian, $\frac{\partial t_0}{\partial t_n}$. Bleistein (1990) assumes that (1) the input data have not been corrected for spherical divergence, (2) NMO is done by resampling without any scale factors, and (3) the spectral density of the input wavelet is preserved. The corresponding value for J_T in Bleistein's algorithm is

$$J_T = A^{-1}(2A^2 - 1)\,. \tag{15}$$

Black et al. (1993) assume that (1) the input data have been corrected for spherical divergence, (2) NMO is done by resampling without any scale factors, and (3) the peak amplitude of the input wavelet is preserved. This leads to the following value for J_T.

$$J_T = A^{-3}(2A^2 - 1)\,. \tag{16}$$

In anisotropic media, the specular reflection point moves differently than in isotropic media. Therefore, the conversion of our algorithm to one honoring amplitudes more

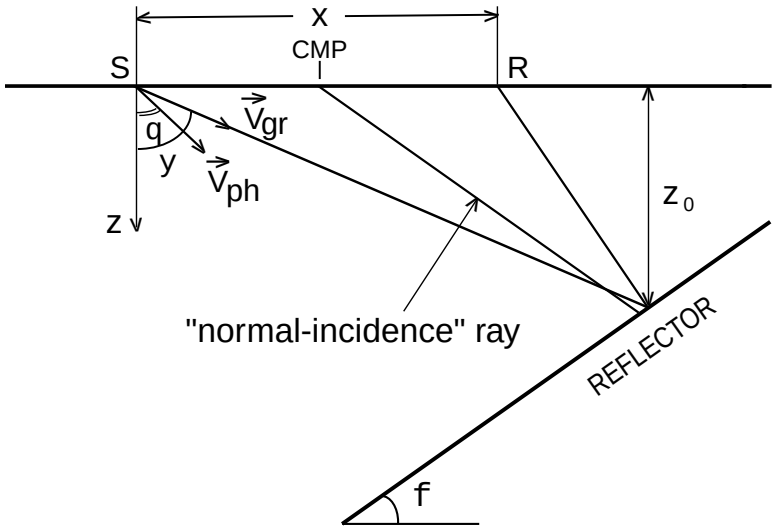

FIG. 1. Common-midpoint gather over a homogeneous anisotropic medium. $\vec{V}_{gr}$ and $\vec{V}_{ph}$ are the group and phase velocity vectors, respectively. The phase-velocity vector corresponding to the zero-offset ray is perpendicular to the reflector.

closely will require the computation of a new Jacobian and phase response specifically for anisotropic media. For the rest of this paper, we will use Hale's Jacobian with an understanding that we are not preserving "true amplitudes" in our processing.

DMO for general anisotropy

Here, we modify Hale's (1984) DMO operator using the anisotropic NMO equation given in Paper I. The model considered in Paper I consists of a planar dipping reflector beneath a homogeneous anisotropic medium (Figure 1). Anisotropy is not restricted to any specific type; however, the incidence (sagittal) plane is supposed to be a plane of symmetry. The most commonly studied anisotropic model for current seismic processing practise is transverse isotropy. For transversely isotropic media, the incidence plane should contain the symmetry axis. If the medium is orthorhombic, the incidence plane should represent one of the mutually orthogonal symmetry planes.

If the symmetry assumption is satisfied, the normal moveout velocity on a CMP line perpendicular to the strike of the reflector is given by (Paper I).

$$V_{\rm nmo}(\phi) = \frac{V(\phi)}{\cos\phi}\,\frac{\sqrt{1+\frac{1}{V(\phi)}\frac{d^2V}{d\theta^2}}}{1-\frac{\tan\phi}{V(\phi)}\frac{dV}{d\theta}}\,, \tag{17}$$

where $V(\theta)$ is phase velocity as a function of phase angle; the derivatives should be evaluated at the dip angle ϕ.

The relation (6) between the dip angle ϕ and ray parameter p on the zero-offset section has the same form in anisotropic media (Paper I).

$$p(\phi) = \frac{1}{2}\frac{dt_0}{dy_0} = \frac{\sin\phi}{V(\phi)} = \frac{k}{2\omega}\,. \tag{18}$$

The replacement of the angle ϕ by the ray parameter p for a known anisotropic model can be done in a straightforward fashion (Alkhalifah and Tsvankin, 1994). The phase angle ϕ and phase velocity $V(\phi)$ corresponding to the horizontal slowness p can be obtained from the Christoffel equation and used in formula (17).

While equation (17) is valid for all wave types, we will consider DMO processing only for P-waves. In order to generalize Hale's DMO for anisotropic media, we need to represent the NMO equation in a form similar to equation (7). Although P-wave reflection moveout even in homogeneous anisotropic media is generally nonhyperbolic (Tsvankin and Thomsen, 1994), it can still be approximated by a hyperbola on spreads with length comparable to the distance between the CMP and the reflector (Paper I).

$$t^2 = t_0^2 + \frac{4h^2}{V_{\rm nmo}^2(p)}\,, \tag{19}$$

with the NMO velocity given by equation (17). Expression (17) is too complicated to be separated analytically into the zero-dip velocity and the DMO correction factor, but we can accomplish this separation artificially by rewriting equation (19) in the same form as equation (4).

$$t_0^2 = t_n^2 + 4h^2\left[\frac{1}{V_{\rm nmo}^2(0)} - \frac{1}{V_{\rm nmo}^2(p)}\right]\,. \tag{20}$$

If the medium is isotropic,

$$V_{\rm nmo}(p) = \frac{V_{\rm nmo}(0)}{\sqrt{1 - p^2 V_{\rm nmo}^2(0)}}\,, \tag{21}$$

and expression (20) reduces to the conventional NMO equation (7).

Therefore, the zero-offset section in anisotropic media can be produced by an NMO-DMO sequence similar to the one used in conventional processing. The zero-dip NMO term $4h^2/V_{\rm nmo}^2(0)$ can be eliminated by the conventional NMO procedure, with the influence of anisotropy hidden in the value of $V_{\rm nmo}(0)$. The only possible complication at this stage is deviations from hyperbolic moveout due to anisotropy. However, as mentioned above, P-wave moveout is sufficiently close to hyperbolic on

conventional spreads where the source-receiver offset is less than or equal to the target depth.

In order to transform the NMO-corrected data to zero offset, the anisotropic DMO operator should compensate for the remaining moveout term $4h^2\,D(p)$ in equation (20), with the factor $D(p)$ given by

$$D(p) = \frac{1}{V_{\rm nmo}^2(0)} - \frac{1}{V_{\rm nmo}^2(p)}\,. \tag{22}$$

The main difference between the anisotropic DMO factor $D(p)$ and its isotropic counterpart p^2 is that $D(p)$ depends on the parameters of the anisotropic velocity field. Therefore, DMO processing should be preceded by an inversion procedure designed to reconstruct the NMO velocity as a function of ray parameter. Clearly, such an inversion is difficult to accomplish for general anisotropy. However, for transverse isotropy with a vertical symmetry axis (VTI), P-wave surface data alone may provide enough information to build the NMO velocity function (Alkhalifah and Tsvankin, 1994). The method developed by Alkhalifah and Tsvankin (1994) is used in our implementation of Hale's DMO in transversely isotropic media.

Assuming that the functions $V_{\rm nmo}(p)$ and $D(p)$ have been recovered and tabulated, the rest of Hale's DMO algorithm remains essentially unchanged. The DMO factor $D(p)$ should be substituted instead of p^2 into the expression for A, yielding the expression valid for anisotropic media in equation (12), with subsequent application of the integral transforms (11) and (8) designed to produce the zero-offset section from the NMO-corrected constant-offset sections. This means that the whole anisotropic NMO-DMO sequence does not take any more computing time than for Hale's method in isotropic media. The only extra step to be included due to the presence of anisotropy is the inversion procedure mentioned above.

Our algorithm ignores anisotropy-induced nonhyperbolic moveout, which seems to be a shortcoming compared to isotropic DMO methods. Although isotropic constant-velocity DMO methods are also based on the hyperbolic moveout equation, they are supposed to work at large offsets because reflection moveout in a homogeneous isotropic medium is purely hyperbolic. However, the homogeneous isotropic model is an idealization of realistic media, which are, at a minimum, vertically inhomogeneous. Any kind of inhomogeneity leads to nonhyperbolic moveout on long spreads that cannot be properly handled by conventional NMO and DMO algorithms.

Also, the results of Paper I and numerical examples discussed below suggest that deviations from hyperbolic moveout usually become less pronounced with dip, at least for transverse isotropy. Therefore, nonhyperbolic moveout can be expected to be more of a problem in the NMO correction for horizontal reflectors than in dip-moveout removal. Also, large offsets at which deviations from a hyperbola are significant, are often muted out because of the NMO stretch. If there is a need to preserve traces at large offsets, DMO processing should be performed by more accurate (but more costly) ray-tracing techniques.

Transversely isotropic media

While the NMO equation (17) can be used in symmetry planes of any anisotropic medium, the main practical difficulty in the implementation of our DMO algorithm in complicated anisotropic models is the recovery of the factor $D(p)$ from seismic data. Therefore, in the following we will concentrate on the most common anisotropic model, transverse isotropy with a vertical symmetry axis (VTI).

As suggested by Thomsen (1986), we describe VTI media by the vertical velocities V_{P0} and V_{S0} of P- and S-waves respectively (we omit the qualifiers in "quasi-P-wave" and "quasi-SV-wave" for brevity) and three dimensionless anisotropic parameters ϵ, δ and γ. It should be emphasized that although the original Thomsen's (1986) paper was devoted to weak transverse isotropy, the parameters ϵ, δ and γ are convenient to use in TI media with arbitrary strength of velocity anisotropy (Tsvankin and Thomsen, 1994; Tsvankin, 1993). In our DMO algorithm we use the exact equations for transverse isotropy without applying the weak-anisotropy assumption.

$P-SV$ propagation depends on four coefficients (V_{P0}, V_{S0}, ϵ, and δ), while the SH-wave velocity is a function of V_{S0} and γ. Tsvankin and Thomsen (1994) proved that P-wave velocities and traveltimes are practically independent of the shear-wave vertical velocity V_{S0}, even for strong anisotropy. Tsvankin (1993) shows that the influence of V_{S0} on the P-wave moveout velocity $V_{\rm nmo}$ is weak, except for the case of strong anisotropy and a wide range of V_{S0}. Therefore, for practical purposes of dip-moveout processing, P-wave NMO velocity can be considered a function of three parameters: V_{P0}, ϵ, and δ.

Due to the trade-off between V_{P0}, ϵ, and δ, these parameters cannot be obtained using only P-wave reflection traveltimes in horizontally-layered VTI models, even if unusually long speads, comparable to two depths of the reflector, are used. However, the need for DMO processing arises only in the presence of dipping reflectors. NMO velocities for reflections from dipping planes provide additional data that put valuable constraints on the model parameters. Alkhalifah and Tsvankin (1994) demonstrate that P-wave NMO velocities from two different dips (e.g., horizontal and dipping reflectors) contain enough information to reconstruct the NMO velocity as a function of ray parameter. The inversion technique, developed by Alkhalifah and Tsvankin (1994), cannot be used to resolve the anisotropies ϵ and δ individually (unless some additional data is available); rather, it is designed to obtain the effective parameter

$$\eta \equiv \frac{\epsilon-\delta}{1+2\delta} = \frac{1}{2}\left[\frac{V_p^2(90)}{V_{\rm nmo}^2(0)} - 1\right], \tag{23}$$

where $V_p(90)$ is the horizontal P-wave phase velocity. It turns out that knowledge of η and the zero-dip NMO velocity $V_{\rm nmo}(0)$ is sufficient to build the function $V_{\rm nmo}(p)$. It is convenient to list the relationships between these elastic parameters in the following form as a memory aid:

$$V_{\rm nmo}(0) = V_{P0}\sqrt{1+2\delta}\,,$$

$$V_P(90) = V_{P0}\sqrt{1+2\epsilon} = V_{\rm nmo}(0)\sqrt{1+2\eta}\,.$$

In order to understand the performance of the anisotropic DMO algorithm, we have to examine the dependence of the factor $D(p)$ on the vertical velocity and anisotropic parameters. First, we consider elliptically anisotropic models, in which wavefronts and slowness surfaces are elliptical for P-waves and spherical for SV-waves. Elliptical anisotropy is a special case of transverse isotropy that occurs if the parameters ϵ and δ are equal to each other.

In elliptically isotropic media, $\epsilon = \delta$, $\eta = 0$, and $V_P(90) = V_{\rm nmo}(0)$. P-wave phase velocity in elliptically anisotropic media is given by

$$V_P(\theta) = V_{P0}\sqrt{1+2\delta\sin^2\theta}\,. \tag{24}$$

The NMO velocity (17) as a function of ray parameter then becomes (Alkhalifah and Tsvankin, 1994)

$$V_{\rm nmo}(p) = \frac{V_{\rm nmo}(0)}{\sqrt{1-p^2V_{\rm nmo}^2(0)}}\,. \tag{25}$$

Equation (25) shows that for elliptical anisotropy P-wave NMO velocity is the same function of the ray parameter and zero-dip moveout velocity as in isotropic media (21), with no explicit dependence on the coefficient $\epsilon = \delta$. The difference between the isotropic and elliptically anisotropic expressions for $V_{\rm nmo}(p)$ is only in the value of the zero-dip velocity $V_{\rm nmo}(0)$, which is equal to the horizontal velocity if the medium is elliptically anisotropic.

Substituting formula (25) into the expression for $D(p)$ (22), we obtain

$$D(p) = p^2\,, \tag{26}$$

which coincides with the DMO factor in the isotropic Hale's algorithm.

We conclude that the constant-velocity Hale's DMO is perfectly suitable not only for isotropic, but also for elliptically anisotropic media. This result is not intuitively clear because the NMO velocity as a function of the dip angle in elliptically anisotropic media deviates from the cosine-of-dip dependence (Paper I). Since reflection moveout for elliptical anisotropy is purely hyperbolic, the whole conventional NMO-DMO sequence should not encounter any problems in elliptical models. The difference between isotropy and elliptical anisotropy becomes important only at the next processing step – poststack migration of the zero-offset section. Since for elliptical anisotropy the zero-dip NMO velocity, conventionally used in migration, does not coincide with the true phase or group velocity in any direction except for horizontal, isotropic post-stack depth migration will result in mispositioning of reflectors, including horizontal

ones (Alkhalifah and Larner, 1994). For horizontal reflectors, the mispositioning is in depth only.

While the elliptical assumption leads to a considerable simplification in the analysis of all aspects of wave propagation, elliptical anisotropy is hardly typical for subsurface formations (Thomsen, 1986). Next, we consider a general transversely isotropic model with no fixed relation between ϵ and δ.

The most convenient way to get analytic insight into the dependence of $D(p)$ on the anisotropic coefficients is to use the weak-anisotropy approximation ($\epsilon \ll 1$, $\delta \ll 1$). The weak-anisotropy formula for the NMO velocity as a function of the dip angle is presented in Paper I. Here, we are interested in a similar expression for the NMO velocity as a function of the ray parameter p.

The P-wave phase velocity, linearized in the parameters ϵ and δ, is given by (Thomsen, 1986)

$$V_P(\theta) = V_{P0}\left(1 + \delta \sin^2\theta \cos^2\theta + \epsilon \sin^4\theta\right). \tag{27}$$

Substitution of equation (27) into the NMO formula (17) and replacement of the phase angle by ray parameter yields (Alkhalifah and Tsvankin, 1994)

$$V^2_{\rm nmo}(p) = \frac{V^2_{\rm nmo}(0)}{1 - p^2 V^2_{\rm nmo}(0)}\left[1 + 2\left(\epsilon - \delta\right) f\left(pV_{\rm nmo}(0)\right)\right], \tag{28}$$

$$f = \frac{y\left(4y^2 - 9y + 6\right)}{1 - y}; \quad y \equiv p^2\, V^2_{\rm nmo}(0)\,.$$

The weak-anisotropy approximation (28) reduces to the exact NMO formula for elliptically anisotropic models [$\epsilon = \delta$, equation (25)] but, certainly, can deviate from the exact result for non-elliptical media.

The DMO correction factor $D(p)$ (22) for weak transverse isotropy becomes

$$D(p) = p^2\left[1 + 2(\epsilon - \delta)\left(4y^2 - 9y + 6\right)\right]. \tag{29}$$

Note that the anisotropic correction to the DMO operator in the weak-anisotropy approximation contains only the difference $\epsilon - \delta$, with no separate dependence on either of the coefficients. The predominant influence of $\epsilon - \delta$ on the dip-dependence of P-wave NMO velocity was shown in Paper I. It is interesting, however, that the weak-anisotropy NMO formula derived in Paper I as a function of the dip angle did contain separate contributions of ϵ and δ. As demonstrated by equations (28) and (29), these contributions are absorbed by the ray parameter p.

The numerical analysis by Alkhalifah and Tsvankin (1994) shows that the structure of the factor $D(p)$ (22) for transverse isotropy with arbitrary strength of velocity

anisotropy is similar to that in equation (29), with the influence of the anisotropies given by the effective parameter η [equation (23)]. Clearly, η reduces to $\epsilon - \delta$ in the limit of weak anisotropy.

Although it might be dangerous to use the weak-anisotropy approximation for quantitative estimates, it is clear from equation (29) that the anisotropy makes a significant contribution to the DMO factor. For instance, for $y = 0.25$, which roughly corresponds to a dip angle of 30°, the anisotropic term $2(\epsilon - \delta)\ (4y^2 - 9y + 6)$ becomes $8(\epsilon - \delta)$, which means that the isotropic and anisotropic parts of the DMO factor are comparable even for relatively small $(\epsilon - \delta)$. This conclusion is in good agreement with results of Paper I.

It is also important that the influence of the anisotropy cannot be ignored even at mild dips; in fact, the relative magnitude of the anisotropic term decreases with dip (with increasing y). Also note that, although the anisotropic DMO operator does depend on the zero-dip NMO velocity through y, the influence of $V_{\rm nmo}(0)$ for any given p is not pronounced, except for large p corresponding to steep dips.

NUMERICAL IMPLEMENTATION

The DMO technique for VTI media discussed above has been implemented using a conventional Hale F-K DMO algorithm. First, $V_{\rm nmo}(\phi)$ and $p = \sin\phi/V(\phi)$ are tabulated from 0 to 89° in constant increments of ϕ for 8000 values using equation (17). Currently, the code allows the entry of the anisotropic coefficients ϵ and δ, the vertical P-wave velocity V_{P0} and the vertical S-wave velocity V_{S0} (the influence of V_{S0}, as mentioned above, is insignificant). Alternatively, we can use η by coding $\delta = 0$ and letting $\epsilon = \eta$. We use the exact equations for NMO and phase velocity for transverse isotropy, so there are no restrictions requiring weak anisotropy in the generation of this table.

Then, that table is interpolated back to a new table of 8000 values in constant increments in p and stored. Based upon this table, $V_{\rm nmo}(p)$ and $D(p)$ can be readily obtained. Input NMO-corrected common-offset data are Fourier-transformed over the midpoint axis providing complex-valued traces as a function of wavenumber. The time integral over t_n is computed numerically yielding the zero-offset section in $\omega - k$ domain.

$$P_0(\omega, k, h) = \int dt_n P_n(t_n, k, h) A^{-1} e^{i\omega t_n A}\,, \tag{30}$$

where $p = \frac{k}{2\omega}$, and

$$A(t_n, k, \omega) = \sqrt{1 + \frac{4h^2}{t_n^2}\left[\frac{1}{V_{\rm nmo}^2(0)} - \frac{1}{V_{\rm nmo}^2(p)}\right]}\,. \tag{31}$$

Finally, a two-dimensional Fourier transform is used to produce the output DMO-corrected common-offset gather in the t-x domain.

SYNTHETIC EXAMPLES

Figures 2-7 demonstrate basic aspects of the transversely isotropic DMO operator compared with isotropic DMO. As expected, the TI DMO algorithm produces results identical to conventional Hale DMO (Figure 2) if the medium is isotropic (Figure 3). Currently, our VTI DMO code is based on Hale's Jacobian. Bleistein's "true amplitude" operator (Figure 4) has the the same shape as Hale's operator but produces a stronger response for the steeper dips.

In agreement with the analytic results discussed above, the transversely isotropic operator reduces to the conventional Hale's operator not only for isotropic but also for elliptically anisotropic media ($\epsilon = \delta$, Figure 5). Although velocity anisotropy for the model in Figure 5 is quite pronounced, it has no influence on the kinematics of the DMO process. The only difference between the two DMO operators is that in the Hale's algorithm the NMO velocity is generated analytically while the VTI DMO response uses the values of $V_{\rm nmo}$ from table lookup.

However, even relatively small deviations from elliptical anisotropy have strong influence on the DMO response. Figure 6 demonstrates the stretching of the DMO ellipse that occurs for a typical transversely isotropic model with positive $\epsilon - \delta$.

The weak-anisotropy approximation was used to compute the impulse response in Figure 7 for the same anisotropic parameters as in Figure 6. For this model, the DMO responses are similar whether or not the weak-anisotropy approximation is used. However, the accuracy of the weak anisotropy approximation decreases for larger values of $\epsilon - \delta$, and we do not use the weak-anisotropy approximation in our routine numerical work.

The next example shows the performance of the VTI DMO algorithm in a homogeneous TI model (V_{P0}=3 km/s, ϵ=0.2, and δ=0.05) with five reflectors, each made up of a dipping segment on the left that connects to a flat interface on the right. The dipping segments have dips of 30, 45, 60, 75, and 90 degrees going from shallow to deep. Figure 8 shows a zero-offset section generated by a ray-tracing algorithm, which may be considered as the ideal output for NMO followed by DMO.

We start our processing using ray-traced common-offset model data (Figure 9). First, common-offset sections are corrected for normal moveout using the actual NMO velocity for horizontal reflectors (Figure 10). Figures 11 and 12 display the zero-offset sections produced by the conventional isotropic Hale's DMO and our transversely-isotropic DMO algorithm respectively. Comparison with the true zero-offset section in Figure 8 shows that the anisotropic DMO algorithm has resulted in a more accurate section.

The differences are more obvious on common-midpoint gathers after NMO and DMO. The NMO corrected CMP gather at midpoint location 3.8 km is shown in Figures 13 and 14, after isotropic DMO and TI DMO respectively. In Figure 14 the events out to a fairly large offset have been aligned, irrespective of dip, allowing CMP stack to sum without distortion. In contrast, after application of isotropic DMO all

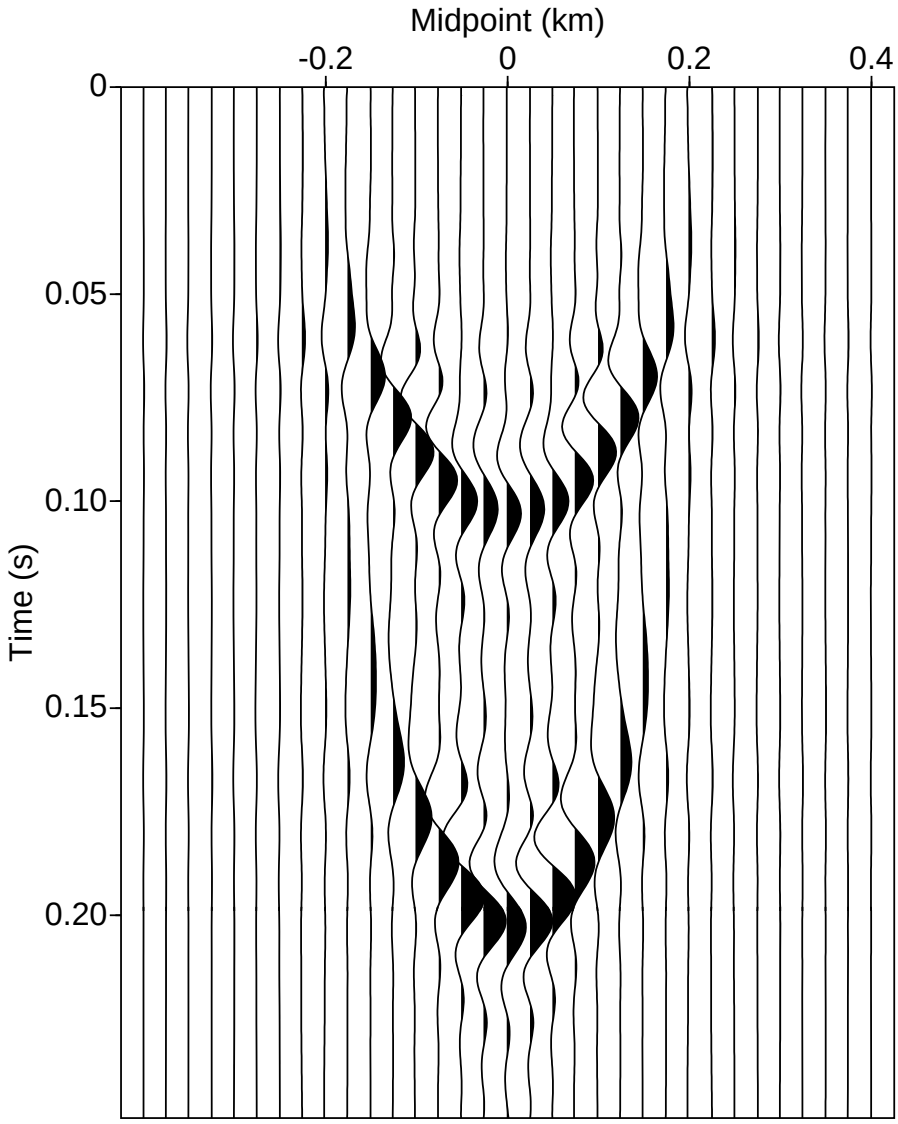

FIG. 2. Isotropic Hale DMO impulse-response curves on a common-offset gather. The offset equals 400 m and the trace spacing is 25 m.

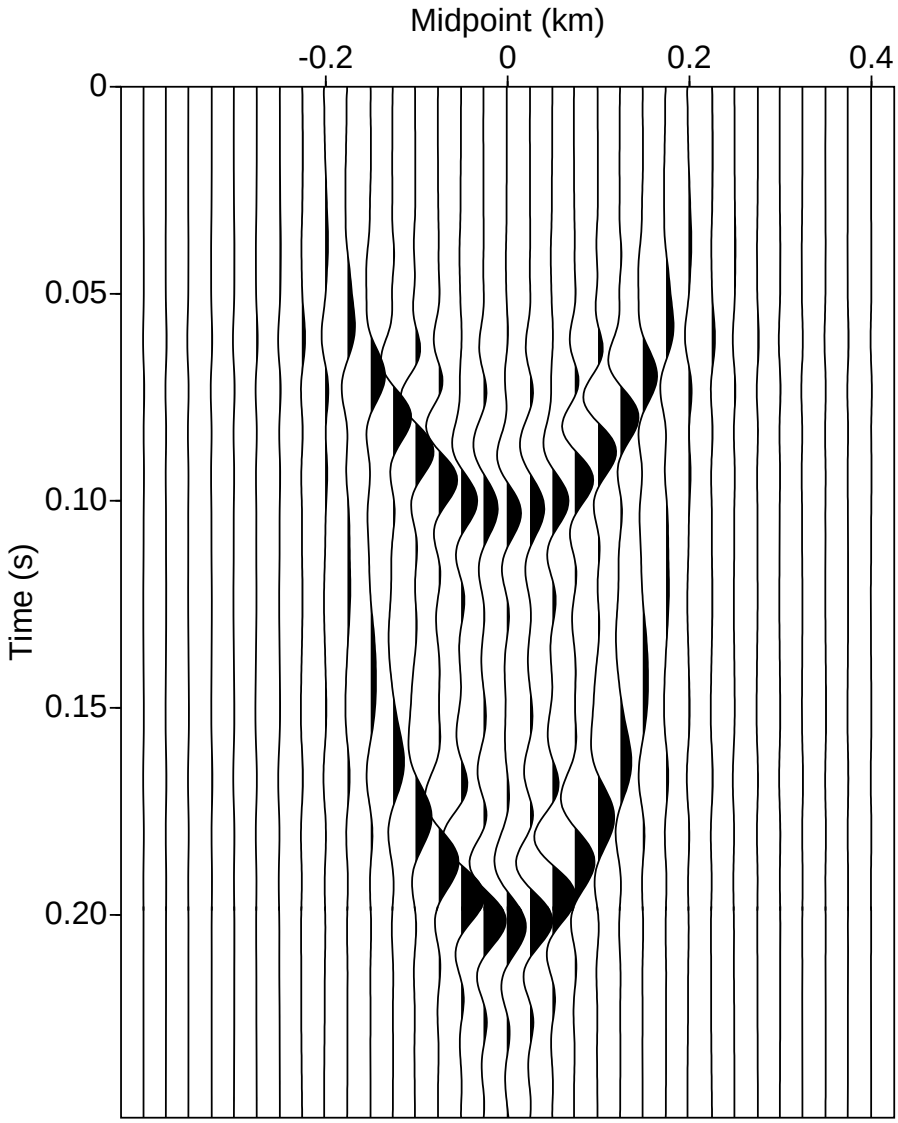

FIG. 3. Isotropic Tsvankin DMO impulse-response curves on a common-offset gather. The offset equals 400 m and the trace spacing is 25 m. This plot demonstrates that the isotropic Tsvankin DMO response is identical to the Hale response.

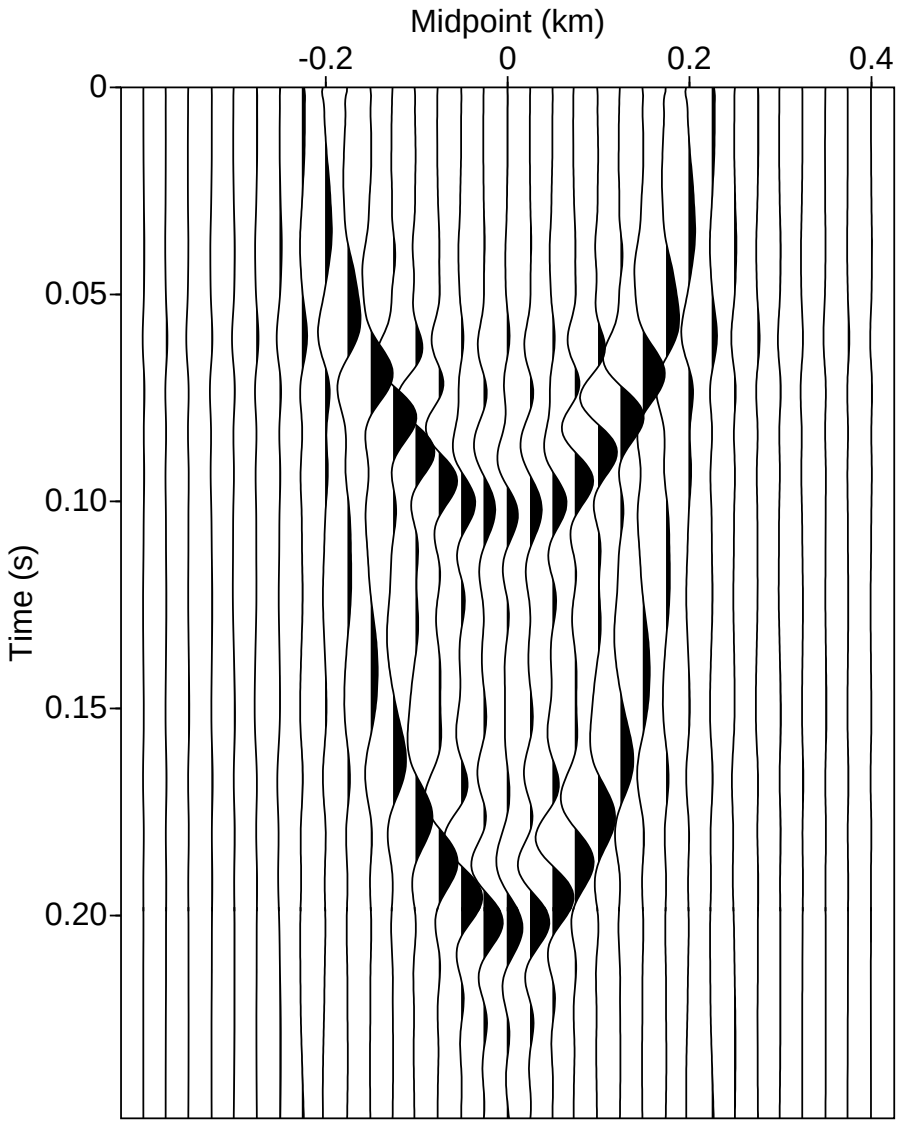

FIG. 4. Isotropic Bleistein DMO impulse-response curves on common-offset gather. The offset equals 400 m and the trace spacing is 25 m. This plot demonstrates that the Bleistein true amplitude DMO response has the same general shape but stronger amplitudes on the steeper dips.

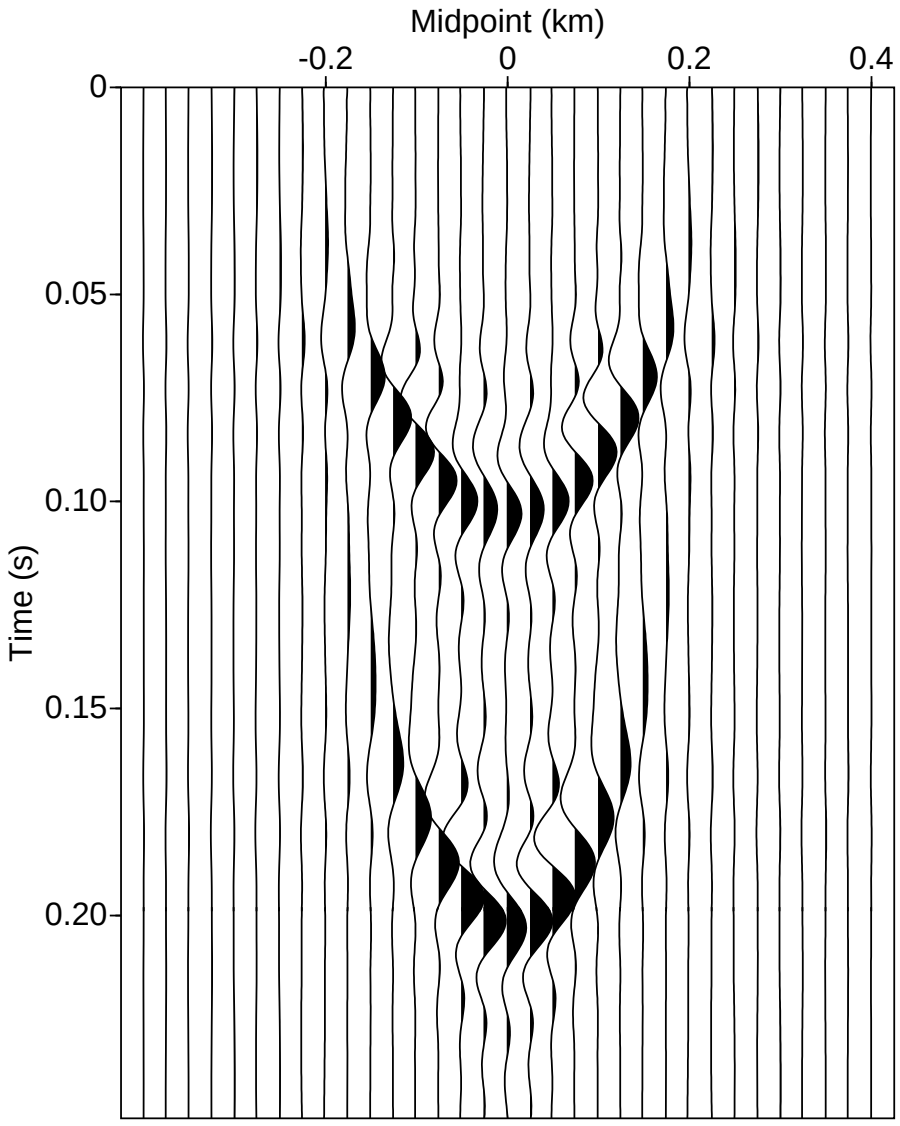

FIG. 5. VTI Tsvankin DMO impulse-response curves on common-offset gather for strong elliptical anisotropy where $\delta = \epsilon = 0.2$. The offset equals 400 m and the trace spacing is 25 m. This figure demonstrates how the elliptically anisotropic DMO operator is almost identical to the isotropic DMO operator for any strength of anisotropy.

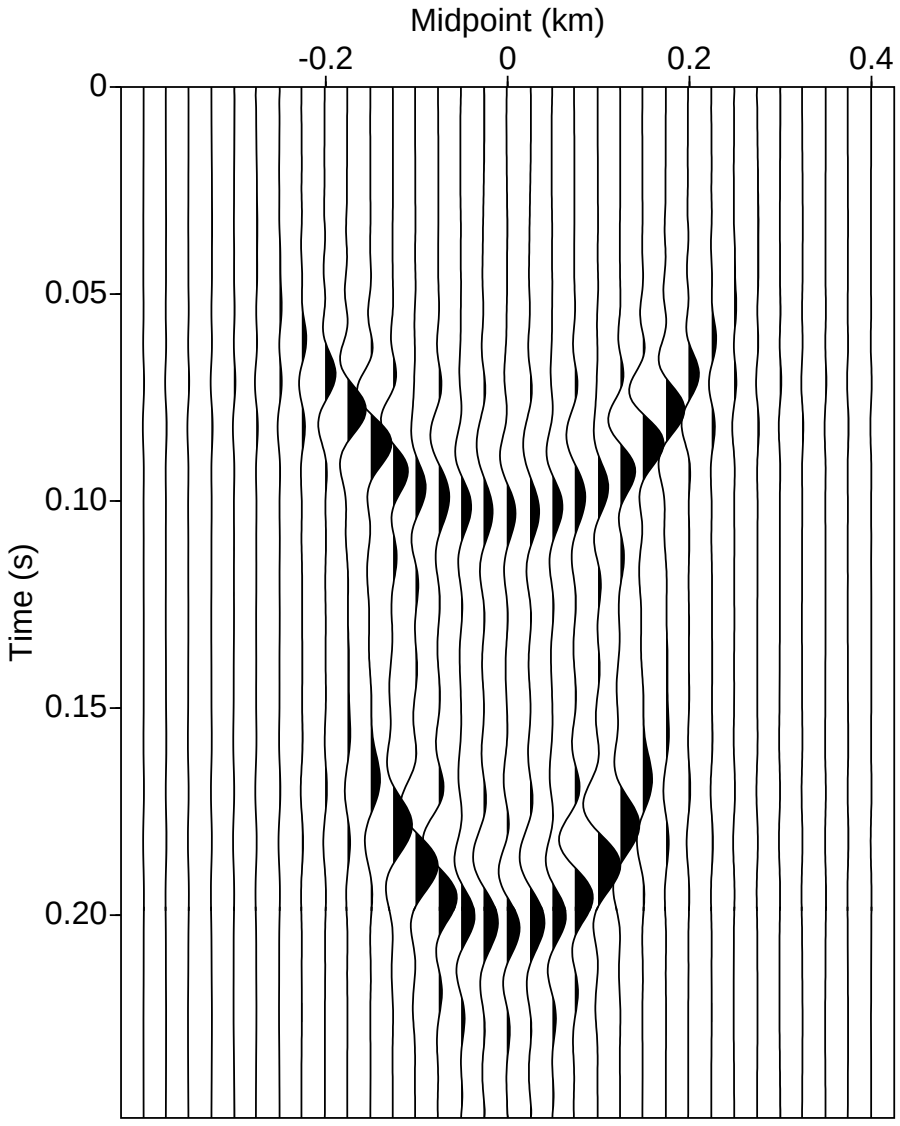

FIG. 6. VTI Tsvankin DMO impulse-response curves on common-offset gather for $\epsilon = 0.2$ and $\delta = 0.1$. The offset equals 400 m and the trace spacing is 25 m. This figure demonstrates that the anisotropic DMO operator spreads out for positive values of $\epsilon - \delta$.

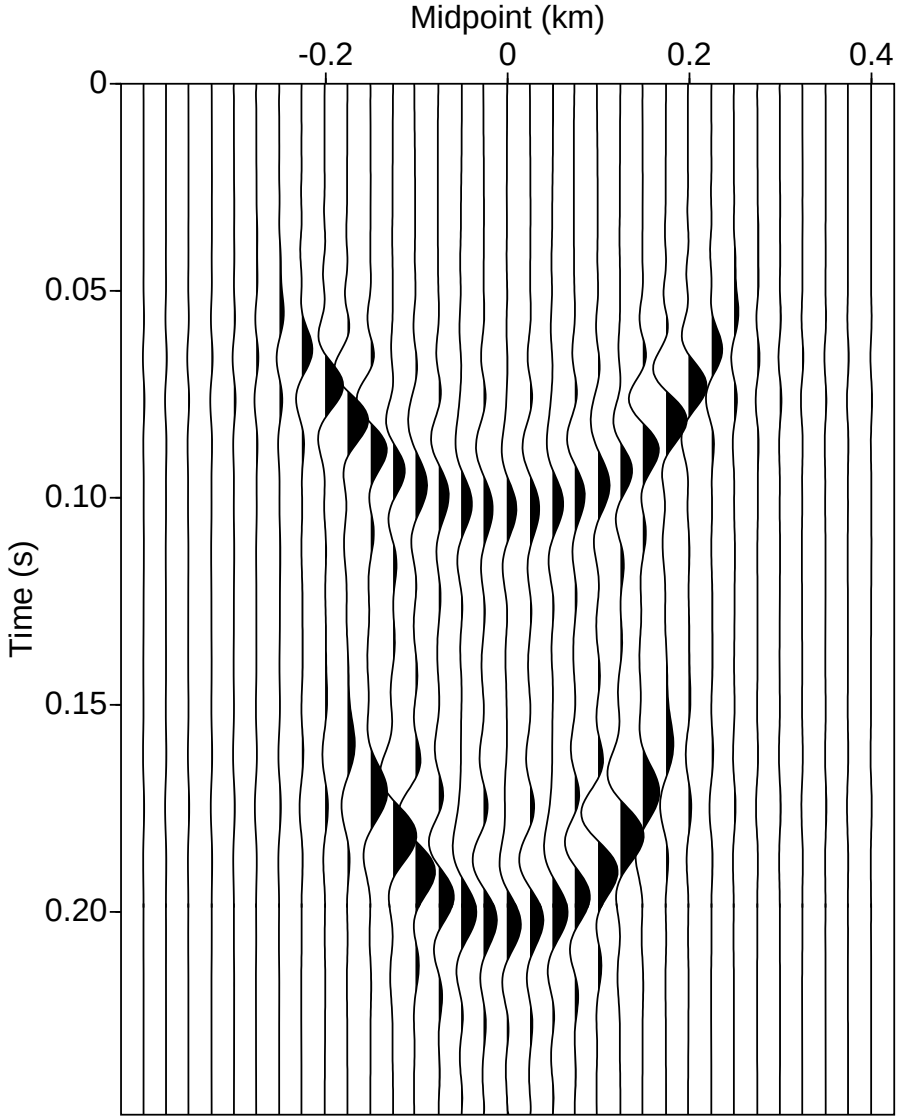

FIG. 7. Using the weak-anisotropy approximation to compute VTI Tsvankin DMO impulse-response curves on common-offset gather for $\epsilon = 0.2$ and $\delta = 0.1$. The offset equals 400 m and the trace spacing is 25 m. Compare to the previous figure.

dipping events remain misaligned. It should be emphasized that the synthetic data were generated by a ray-tracing algorithm that is not related to the analytic formula used in our TI DMO correction.

Figure 14 points out several additional features. The horizontal events still have significant nonhyperbolic moveout and will require muting on the longer offsets prior to the stack. The dipping events also have nonhyperbolic moveout, but to a far lesser degree than the horizontal events. If it is necessary to include very long offsets in the stack, an NMO/DMO sequence based on anisotropic ray tracing will be necessary to correct for nonhyperbolic moveout.

DISCUSSION AND CONCLUSIONS

Hale's DMO method has been extended to anisotropic media using the analytic expression for NMO velocity given by Tsvankin (1993). For elliptical anisotropy ($\epsilon = \delta$), the isotropic DMO algorithm remains entirely valid, although poststack depth migration based on the zero-dip moveout velocity may result in depth errors. However, elliptical anisotropy is just a special kind of transverse isotropy that cannot be considered as typical for subsurface formations, and even relatively small deviations from the elliptical model may result in significant DMO errors.

The anisotropic correction to the DMO operator for general transversely isotropic media is determined by two effective parameters: the anisotropic coefficient $\eta = (\epsilon - \delta)/(1 + 2\delta)$ and the NMO velocity for a horizontal reflector. A robust technique designed to recover both parameters from surface P-wave data has been developed by Alkhalifah and Tsvankin (1994). After the inversion step has been completed, an analytic moveout equation (Tsvankin, 1993) is used to tabulate the NMO velocity as a function of the ray parameter. Then we carry out the transformation of constant-offset sections to zero offset essentially in the same fashion as in isotropic media. Except for the inversion procedure, the whole NMO-DMO sequence does not take more computing time than in isotropic media.

Knowledge of η and $V_{\rm nmo}(0)$ is sufficient not only for DMO, but for all kinds of time processing such as prestack and poststack migration. However, accurate time-to-depth conversion requires the individual values of the vertical velocity V_{P0} and anisotropic parameters ϵ and δ. The current version of our DMO code operates with ϵ and δ, but it is easy to switch to the effective parameter η by setting $\delta = 0$, $\epsilon = \eta$.

Tests of the algorithm on synthetic data for transversely isotropic media show that it efficiently flattens the short-spread moveout, independent of dip. Two interesting points are clarified by the examples. First, reflections from steep interfaces are less effected by nonhyperbolic moveout and often appear flatter after DMO than are those from horizontal reflectors. This conclusion in good agreement with the results reported by Tsvankin (1993). Second, the DMO response of this algorithm in strongly anisotropic media is not restricted to the region between the source and the receiver.

The DMO technique described here assumes that the offset-to-target-depth ratio

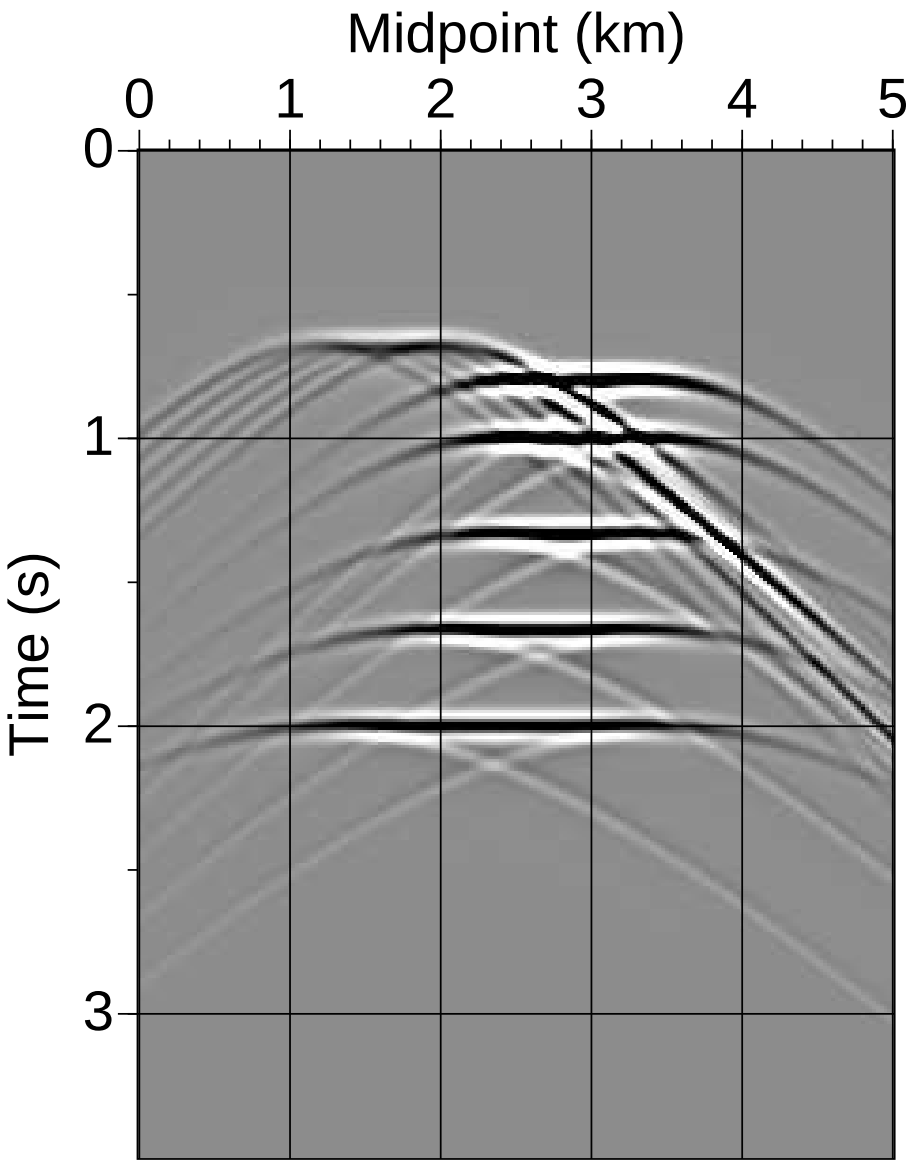

FIG. 8. Zero-offset section generated by ray tracing in a homogeneous TI model with $V_{P0} = 3$ km/s, $\epsilon = 0.2$, and $\delta = 0.05$. Five reflectors with 30, 45, 60, 75, and 90 degree dips intersect corresponding horizontal reflectors at depths of 1.2, 1.5, 2.0, 2.5, and 3.0 km, respectively.

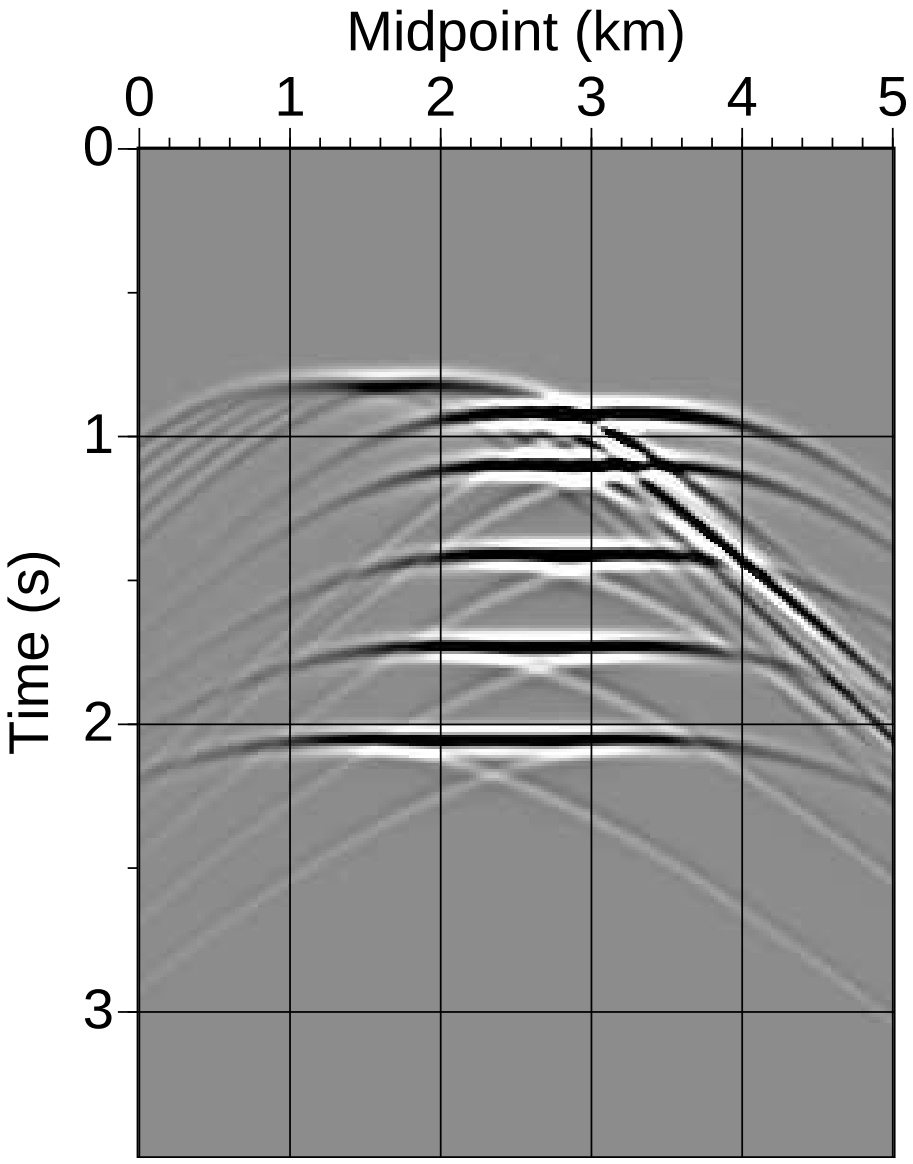

FIG. 9. Common-offset (1.5 km) section for the TI model from Figure 8.

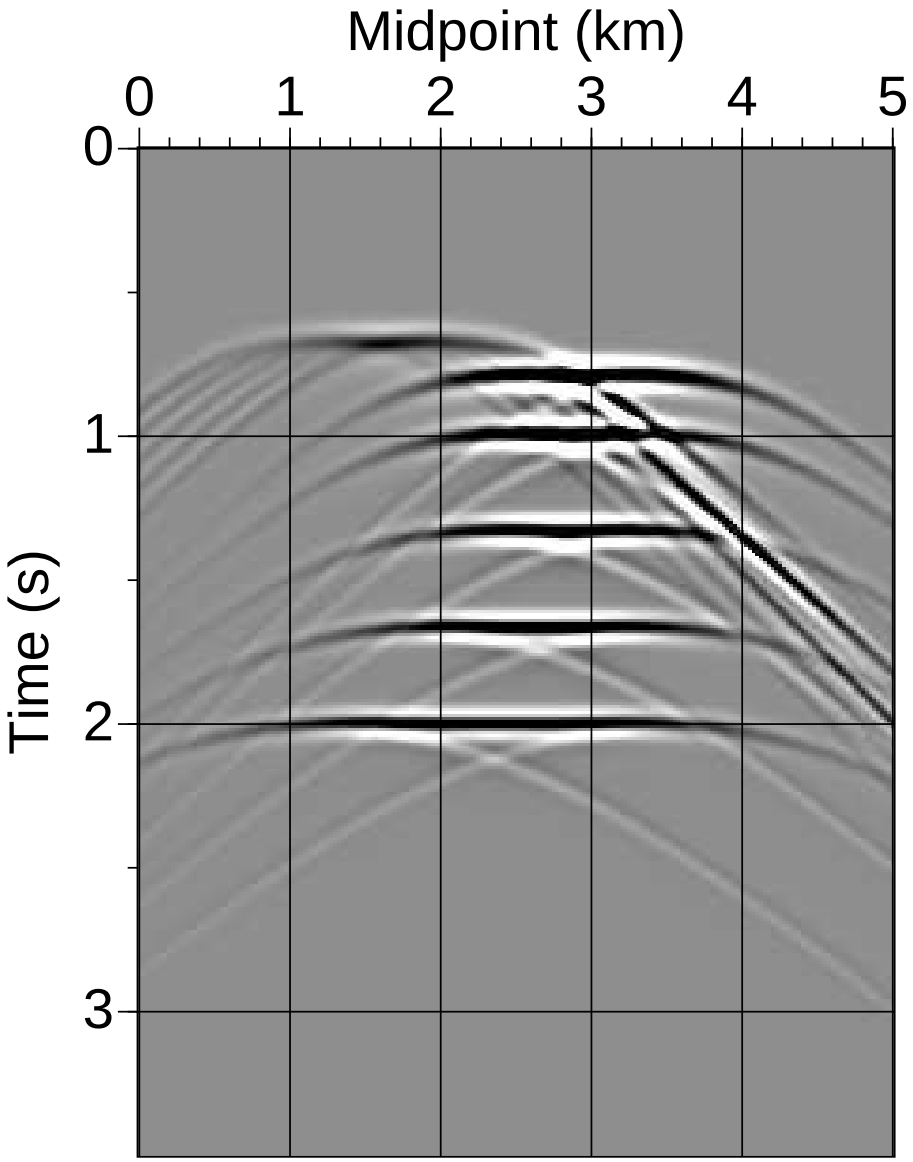

FIG. 10. Common-offset (1.5 km) section from Figure 9 after the normal-moveout correction using the true NMO velocity for horizontal reflectors (2098 m/s).

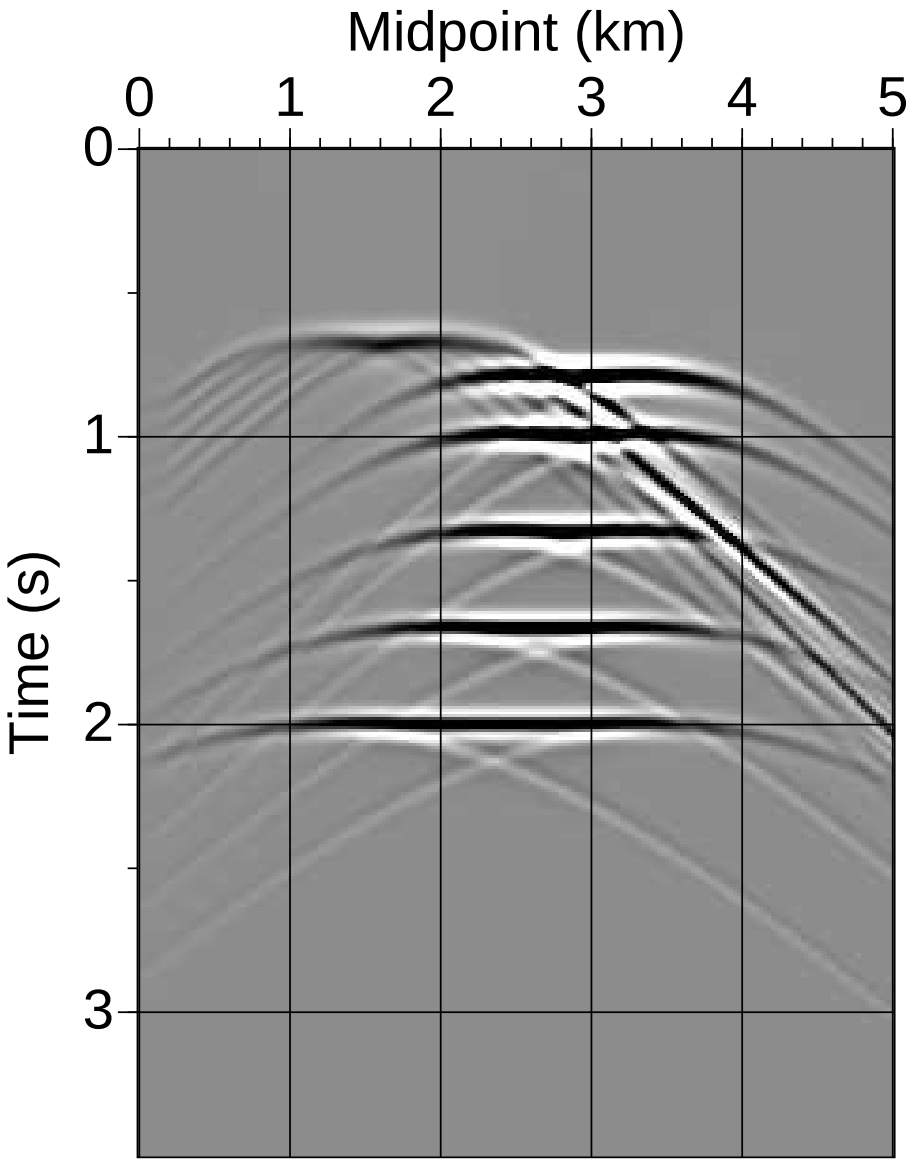

FIG. 11. NMO-corrected common-offset (1.5 km) section from Figure 10 after isotropic DMO. Compare with the true zero-offset section in Figure 8 and with the TI DMO result in Figure 12.

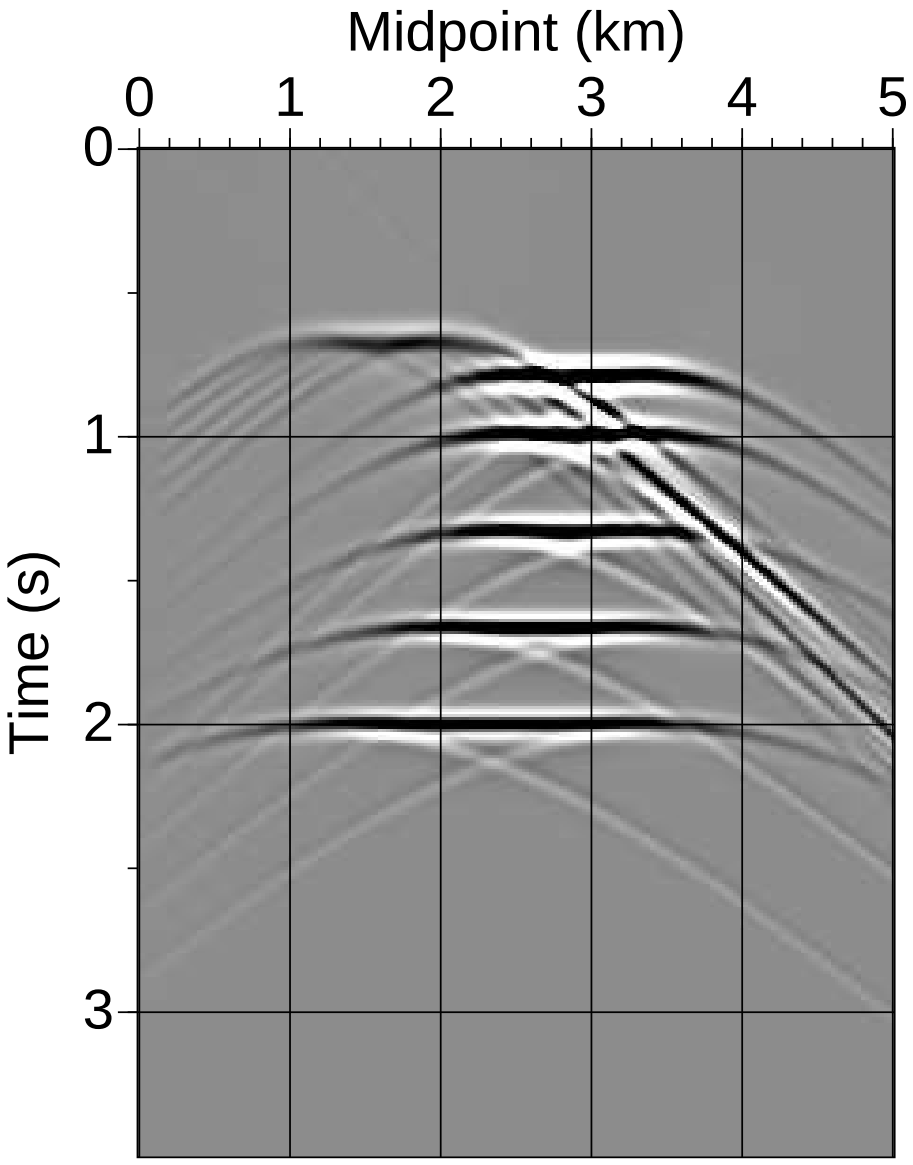

FIG. 12. NMO-corrected common-offset (1.5 km) section from Figure 10 after TI DMO. Compare with the true zero-offset section in Figure 8 and with the isotropic DMO result in Figure 11.

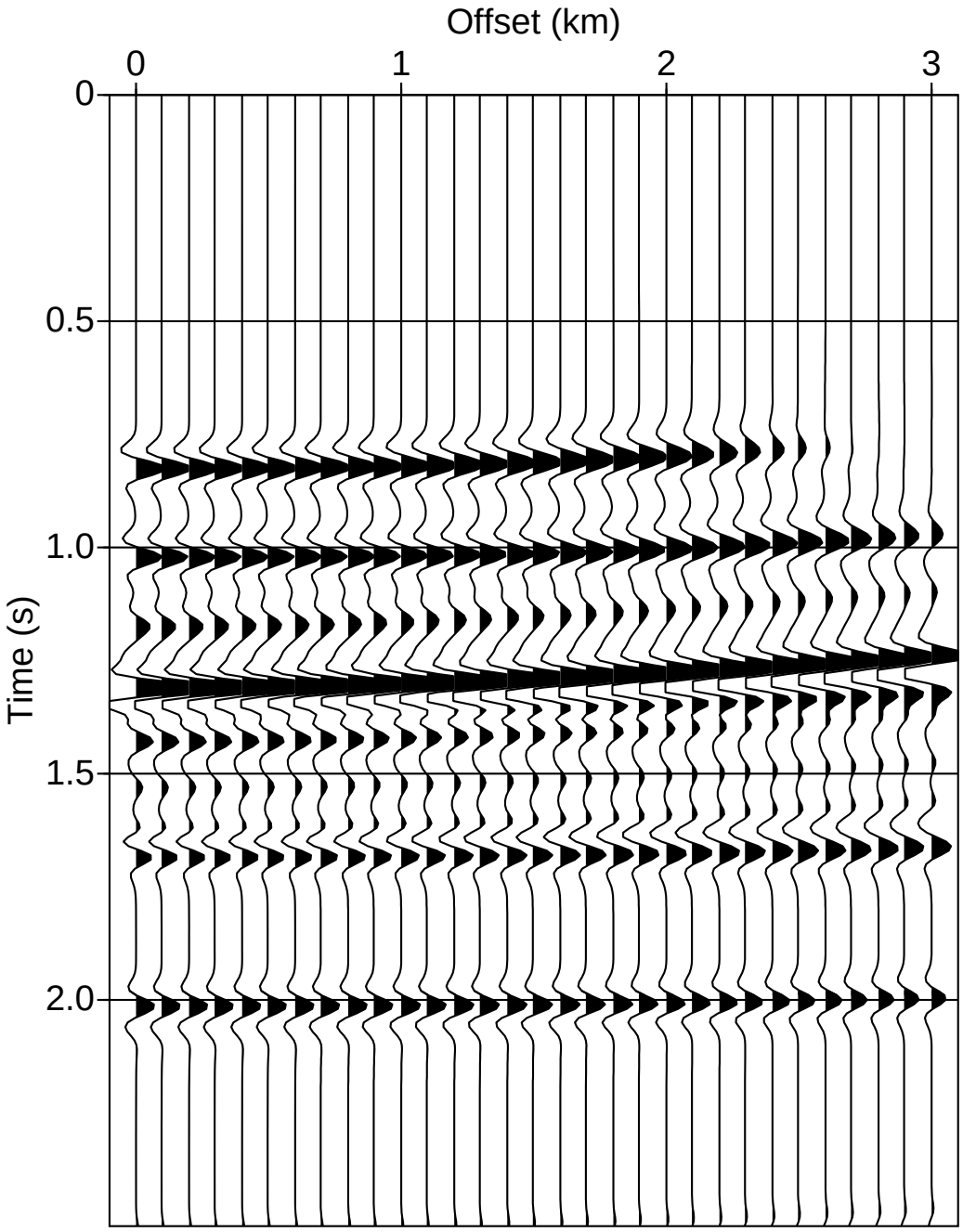

FIG. 13. CMP gather after NMO and isotropic DMO at midpoint location 3.8 km. Ideally all the events should be perfectly flat and ready to stack. However, isotropic DMO leaves residual curvature on some events. All reflection events are peaks colored in black. The top two events at .8 and 1.1 s are diffractions from 0 degree dips. The events at 1.2, 1.3, and 1.4 s are from 30, 45 and 0 degree dips respectively. Just below 1.5 s are two weak events from dips of 60 and 75 degrees respectively followed by two diffractions from horizontal reflectors.

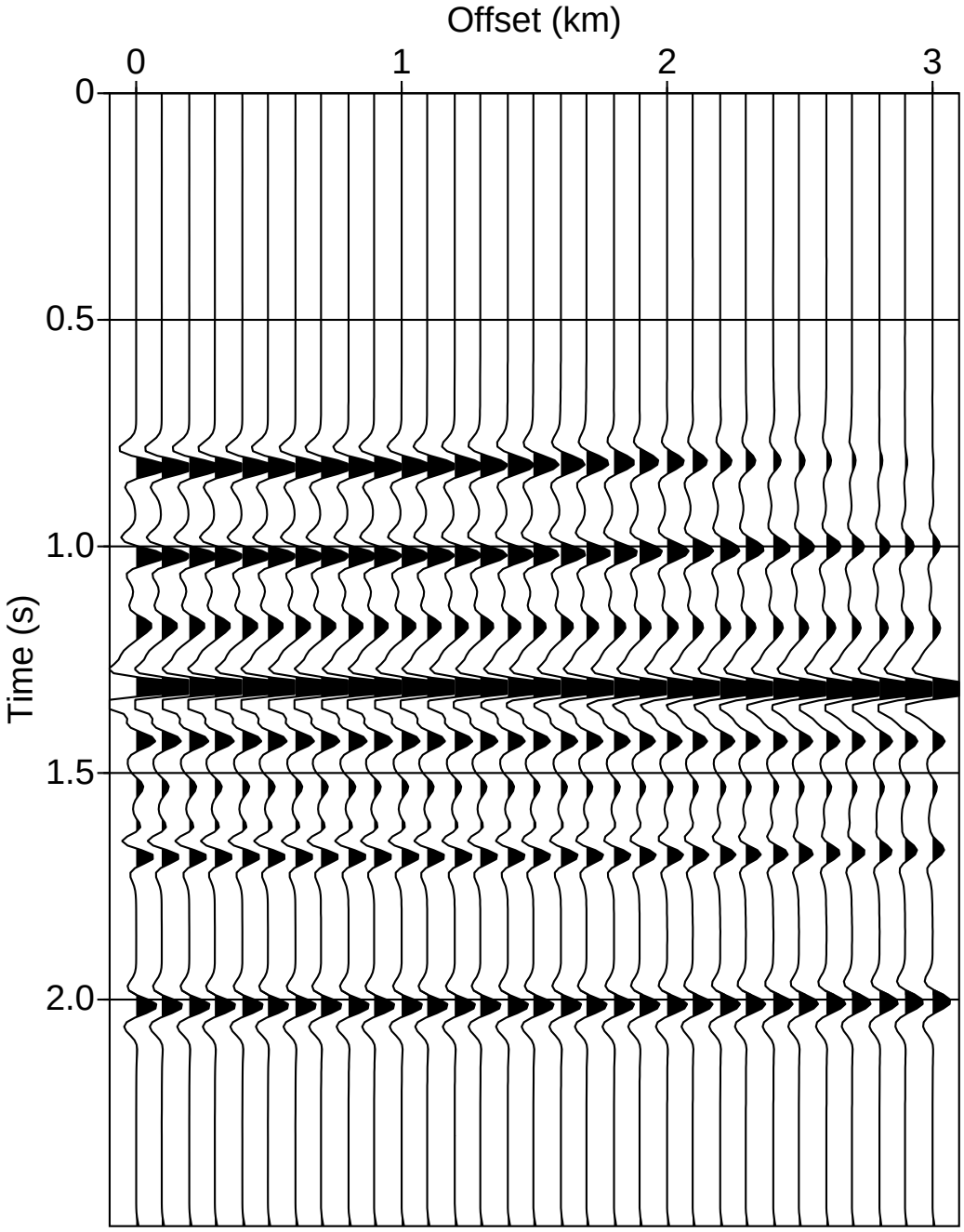

FIG. 14. CMP gather after NMO and TI DMO at midpoint location 3.8 km. TI DMO has flattened the data out to fairly large offsets far more effectively than has isotropic DMO. There is some residual curvature on the far offset events due to non-hyperbolic moveout. This algorithm is effective only for the offset range where the moveout is hyperbolic. In general, the non-hyperbolic moveout appears much weaker on the reflections from dipping reflectors.

is less than one and does not correct for nonhyperbolic moveout. Therefore, practical use may require a careful initial mute as a function of offset on the data after NMO and DMO but prior to CMP stacking. However, as mentioned above, in typical TI models deviations from hyperbolic moveout become less pronounced with dip, so we expect nonhyperbolic moveout to be more of a problem in normal-moveout correction than in DMO.

Our anisotropic DMO operator can be applied in a straighforward way in symmetry planes of more complicated models such as orthorhombic. The main problem in DMO processing for anisotropic models with a large number of independent parameters is the reconstruction of the dip-dependence of NMO velocity from seismic data. The algorithm can be upgraded to perform $V(z)$ DMO by replacing the single-layer NMO formula with a more general equation for layered media developed by Alkhalifah and Tsvankin (1994). In the future, we will also explore the possibility of using the log-stretch trick to increase the computational efficiency of the new DMO technique.

ACKNOWLEDGMENTS

We are grateful to Ken Larner (CSM), Tariq Alkhalifah (CSM), and Denis Schmitt (Mobil) for helpful discussions and suggestions. This work was performed during John Anderson's tenure as the Mobil Visiting Scientist in the Department of Geophysics at the Colorado School of Mines.

REFERENCES

Alkhalifah, T., and Larner, K., 1994, Migration errors in transversely isotropic media: Submitted to Geophysics.

Alkhalifah, T., and Tsvankin, I., 1994, Velocity analysis for transversely isotropic media: This volume.

Banik, N.C., 1984, Velocity anisotropy of shales and depth estimation in the North Sea basin: Geophysics, **49**, 1411-1419.

Black, J.L., Schleicher, K.L., and Zhang, L., 1993, True-amplitude imaging and dip moveout: Geophysics, **58**, 47-66.

Bleistein, N., 1990, Born DMO revisited: 60th SEG Annual International Meeting, Expanded Abstracts, 1366-1369.

Forel, D., Gardner, G.H.F., 1988, A three-dimensional perspective on two-dimensional dip moveout: Geophysics, **53**, 604-610.

Hale, D., 1984, Dip-moveout by Fourier transform: Geophysics, **49**, 741-757.

Hale, D., and Artley, C., 1993, Squeezing dip moveout for depth-variable velocity: Geophysics, **58**, 257-264.

Larner, K., 1993, Dip-moveout error in transversely isotropic media with linear velocity variation in depth: Geophysics, **58**, 1442-1453.

Levin, F.K., 1971, Apparent velocity from dipping interface reflections: Geophysics, **36**, 510-516.

Levin, F.K., 1990, Reflection from a dipping plane - Transversely isotropic solid: Geophysics, **55**, 851-855.

Robertson, J.D., and Corrigan, D., 1983, Radiation patterns of a shear-wave vibrator in a near-surface shale: Geophysics, **48**, 19-26.

Sams, M.S., Worthington, M.H., and Khanshir, M.S., 1993, A comparison of laboratory and field measurements of P-wave anisotropy: Geophysical Prospecting, **41**, 189-206.

Thomsen, L., 1986, Weak elastic anisotropy: Geophysics, **51**, 1954-1966.

Tsvankin, I., 1993, Analytic description of dip moveout in anisotropic media: CWP Annual Project Review, CSM (also submitted to Geophysics).

Tsvankin, I.D., and Thomsen, L.A., 1994, Nonhyperbolic reflection moveout in anisotropic media: Geophysics, in press.

Uren, N.F., Gardner, G.H.F., and McDonald, J.A., 1990a, Dip moveout in anisotropic media: Geophysics, **55**, 863-867.

White, J. E., Martineau-Nicoletis, L., and Monash, C., 1983, Measured anisotropy in Pierre Shale: Geophys. Prosp., **31**, 709-725.